



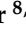





Article

Bioremediation of Battery Scrap Waste Contaminated Soils Using Coco Grass (*Cyperus rotundus* L.): A Prediction Modeling Study for Cadmium and Lead Phytoextraction

Arwa A. AL-Huqail ¹, Mostafa A. Taher ², Ivan Širić ³, Madhumita Goala ⁴, Bashir Adelodun ^{5,6}, Kyung Sook Choi ⁶, Piyush Kumar ⁷, Vinod Kumar ⁸, Pankaj Kumar ^{8,*} and Ebrahim M. Eid ^{9,*}

- ¹ Department of Biology, College of Science, Princess Nourah bint Abdulrahman University, P.O. Box 84428, Riyadh 11671, Saudi Arabia
 - ² Biology Department, Faculty of Science and Arts, King Khalid University, Mohail Assir 61321, Saudi Arabia
 - ³ Faculty of Agriculture, University of Zagreb, Svetosimunska 25, 10000 Zagreb, Croatia
 - ⁴ Department of Environment Science, Graphic Era (Deemed to be University), Dehradun 248002, India
 - ⁵ Department of Agricultural and Biosystems Engineering, University of Ilorin, PMB 1515, Ilorin 240103, Nigeria
 - ⁶ Department of Agricultural Civil Engineering, Kyungpook National University, Daegu 41566, Republic of Korea
 - ⁷ Department of Science, Vivek College of Education, Moradabad Road, Bijnor 246701, India
 - ⁸ Agro-Ecology and Pollution Research Laboratory, Department of Zoology and Environmental Science, Gurukula Kangri (Deemed to be University), Haridwar 249404, India
 - ⁹ Botany Department, Faculty of Science, Kafrelsheikh University, Kafr El-Sheikh 33516, Egypt
- * Correspondence: rs.pankajkumar@gkv.ac.in (P.K.); ebrahim.eid@sci.kfs.edu.eg (E.M.E.)



Citation: AL-Huqail, A.A.; Taher, M.A.; Širić, I.; Goala, M.; Adelodun, B.; Choi, K.S.; Kumar, P.; Kumar, V.; Kumar, P.; Eid, E.M. Bioremediation of Battery Scrap Waste Contaminated Soils Using Coco Grass (*Cyperus rotundus* L.): A Prediction Modeling Study for Cadmium and Lead Phytoextraction. *Agriculture* **2023**, *13*, 1411. <https://doi.org/10.3390/agriculture13071411>

Academic Editor: Fernando P. Carvalho

Received: 29 May 2023

Revised: 7 July 2023

Accepted: 14 July 2023

Published: 16 July 2023



Copyright: © 2023 by the authors. Licensee MDPI, Basel, Switzerland. This article is an open access article distributed under the terms and conditions of the Creative Commons Attribution (CC BY) license (<https://creativecommons.org/licenses/by/4.0/>).

Abstract: With the increasing demand for electronic devices that use batteries, e-waste is also becoming a major threat to the environment. Battery e-waste contains hazardous heavy metals that affect the health of the soil ecosystem. Thus, the present study evaluates the cadmium (Cd) and lead (Pb) phytoextraction potential of coco grass (*Cyperus rotundus* L.) grown in soils contaminated with battery scrap waste (BSW). Pot experiments were conducted to grow *C. rotundus* under different treatments (0%: control, T1: 1%, T2: 2%, T3: 3%, and T4: 4%) of BSW mixed with soil (*w/w*). The results showed that BSW mixing significantly ($p < 0.05$) increased the physicochemical properties and heavy metal (Cd and Pb) content in the soil. BSW mixing resulted in a reduction in growth and biochemical traits of *C. rotundus* and an increase in oxidative stress enzymes with an increase in BSW dose. The Pearson correlation studies also showed that soil HM concentration had a negative influence on the growth and biochemical parameters of *C. rotundus*. The bioaccumulation and translocation factor analysis showed that *C. rotundus* was a hyperaccumulator plant with a maximum accumulation of Cd and Pb (38.81 and 109.06 mg·kg⁻¹) in root parts followed by the whole plant (277.43 and 76.10 mg·kg⁻¹) and shoot (21.30 and 22.65 mg·kg⁻¹) parts. Moreover, predictive models based on multiple linear regression (MLR) and artificial neural network (ANN) approaches were developed for Cd and Pb uptake by *C. rotundus*. Mathematical modeling results showed that soil properties were useful to construct quality MLR and ANN models with good determination coefficient ($R^2 > 0.98$), model efficiency (ME > 0.99), and low root mean square error (RMSE < 5.72). However, the fitness results of the ANN models performed better compared with those of the MLR models. Overall, this study presents an efficient and sustainable strategy to eradicate hazardous HMs by growing *C. rotundus* on BSW-contaminated soils and reducing its environmental and health consequences.

Keywords: hazardous waste; heavy metals; mathematical models; phytoremediation; soil pollution; waste management

1. Introduction

Batteries are devices that convert stored chemical energy into electrical energy, which can be used to power electronic devices [1]. Different types of batteries, such as nickel-cadmium (Ni-Cd), lead-acid (Pb-acid), lithium-ion (Li-ion), zinc-carbon (Zn-C), etc., are used in various sectors, including commercial, communication, transportation, and household [2]. It is estimated that the global battery market shared approximately USD 104.31 billion in 2022 with a >15% of compound annual growth rate (CAGR). The revenue of the battery market is expected to hit USD 329.84 billion by 2030 [3]. India imported more than 0.62 million tons of Ni-Cd-based ores during 2017–2018 to meet its battery production demands [4]. However, the management of spent batteries has continued to become a serious environmental issue since the efficiency of these batteries is reduced after a certain period and the batteries need to be discarded. In the last decades, rapid industrialization and urbanization have created devastating impacts by releasing hazardous wastes into our environment [5]. Spent BSW is one of the most dangerous hazardous wastes that pollute soil, water, and air [6]. Being hazardous waste, battery scrap waste (BSW) has become a global issue with the rapid growth of electronic devices and electric vehicles worldwide.

With an increasing demand for batteries, the problem of BSW management is also becoming threatening. Developing countries often lack the necessary infrastructure to sustainably manage BSW, which leads to increased environmental and health risks (Guerero et al., 2013). Thus, significant portions of BSW, including metal plates, plastic, straps, intercell connectors, spent electrolytes (acids and bases), etc., end up in landfill rather than being properly recycled [7]. Unsafe disposal and poor recycling of BSW can also lead to several toxic heavy metals (HMs), such as Cd, Pb, Ni, Co, and Li, entering the soil and groundwater continuum [8]. Elevated levels of hazardous HMs in soil and groundwater can inflict significant health damage to humans, animals, plants, and soil microbes [9,10]. In particular, Cd and Pb are reported to cause several respiratory issues, kidney damage, bone osteoporosis, cardiovascular effects, and reproductive and developmental problems, among many others. [11,12]. Plants also experience severe effects of high Cd and Pb stress, such as reduced growth and development, chlorosis, leaf damage, altered mineral balance, oxidative stress, impaired fertilization, and accumulation in edible parts [13,14]. Recent studies have shown that soils impacted by BSW have an extremely high content of Cd and Pb, which requires urgent attention to prevent further movement to upper trophic levels, including human beings [15,16].

Environmentally friendly decontamination of soils impacted by hazardous HMs has become crucial to avoid any health consequences. In recent times, phytoremediation has emerged as one of the best approaches for the efficient removal of several HMs using hyperaccumulator plant species [17]. Several authors reported successful reclamation of soils contaminated with HMs, including those affected by BSW [18], landfill leachate [19], coal mining [20], and copper smelting [21], using hyperaccumulator plants. Such plants respond to physiological stress by sequestering HMs into their vegetative parts, chelating HMs using specialized chelators and transporter molecules, and producing antioxidant enzymes [22,23]. Therefore, these features of plant phytoremediation make them ideal candidates for the bio-extraction of HMs from contaminated soils. Moreover, the efficiency of phytoremediation systems can be enhanced by the use of several mathematical models [24]. The pollutant removal process of plants can be efficiently optimized by regulating several intrinsic and extrinsic factors. For this, different types of mathematical models, such as logistic, multiple linear regression (MLR), artificial neural networks (ANN), etc., are widely used [25].

Cyperus rotundus L., also known as coco grass, nut grass, nut sedge, or java grass, belongs to the family Cyperaceae and is a perennial plant widely found in Africa, South Asia, and central Europe. It is a small plant, considered a weed, that generally reproduces rapidly in moist soils to take over soil fertilizers [26]. It propagates by tubers, basal bulbs, division, and seeds. The tubers sprout into numerous rhizomes and expand vertically, forming several roots which radiate horizontally [27]. Tubers are found mostly in the upper

45 cm of the soil surface and can remain unaffected under severe droughts for several years. It is estimated that *C. rotundus* can produce over 10–30 million tubers/ha in one season, which may negatively affect crop production [28]. However, evidence shows that tubers of *C. rotundus* are consumed as a medicinal and staple food by several tribal people in India and Africa [29,30]. Apart from its culinary uses, *C. rotundus* is also utilized for the phytoextraction of HMs from contaminated soils [31]. *C. rotundus* can tolerate high HM stress, thereby providing a solution to the contaminated soil management. Significant bio-extraction of HMs, including Cd, Pb, Zn, and Ni, was reported by Nwaichi et al. [32].

Considering the aforementioned, this study aimed to investigate the Cd and Pb phytoextraction potential of *C. rotundus* grown on BSW-contaminated soils. Laboratory experiments were conducted to understand the effect of different BSW loading rates on growth, biochemical and enzyme response, and HMs accumulation by *C. rotundus*.

2. Materials and Methods

2.1. Experimental Materials

Loam soil was collected from agricultural lands of rural Haridwar, Uttarakhand, India (29°53'13.6" N and 78°08'15.2" E), which was not previously exposed to any industrial or urban activities. The experimental soil was identified as having a loamy texture (clay: 19%, silt: 42%, and sand: 38%) based on the composition of clay, silt, and sand present in it. The mixed type of battery scrap waste (BSW) containing Pb-acid and Ni-Cd batteries was collected from a local scraper near Nakur town, Saharanpur district, Uttar Pradesh, India (29°55'38.6"N and 77°18'58.4"E). The acid and outer case of the batteries were carefully removed and internal parts were dismantled. Then, selected internal components were separated (cells, plates, connectors, and terminal posts) shredded, and converted into fine powder form using a portable industrial shredder with the help of a local scraper. On the other hand, juvenile and healthy rhizomes (2–3 cm in length) of coco grass (*C. rotundus*) were also collected from the soil sampling site by digging 15 cm below the surface. The tubers were washed with tap water to remove adhering soil and collected in 100 gm capacity zip-locking aerated polythene bags and transported to the laboratory for further experiments.

2.2. Experimental Design and Operation

For the present study, phytoremediation experiments were conducted using rectangular plastic pots (35 × 20 × 15 cm; length × width × depth). Each pot was filled with 10 kg arable soil and mixed with an appropriate dose (*w/w*) of BSW—i.e., 0% (no BSW mixing), 1, 2, 3, and 4%, respectively. Figure 1 shows the design of phytoremediation experiments using *C. rotundus*. The soil was loosened to a depth of 8–10 cm in order to promote quick propagation. For each pot, a total of five identical rhizomes were sown in small holes at a depth of 5 cm. The holes were covered with soil and pots were equally watered using a borewell water supply to maintain consistent moisture. Tubers were sown on 1 March 2022 and experiments were terminated after 45 days, i.e., on 14 April 2022. For this, pots were placed under the open sky with a direct sunlight period of 10 h and natural environmental conditions. The tubers were allowed to sprout, and seedlings emerged within 15 days, followed by 30 days of vegetative plant growth. The plants were irrigated twice a week with borewell water, and other emerging weeds were immediately removed to avoid any experimental inference.

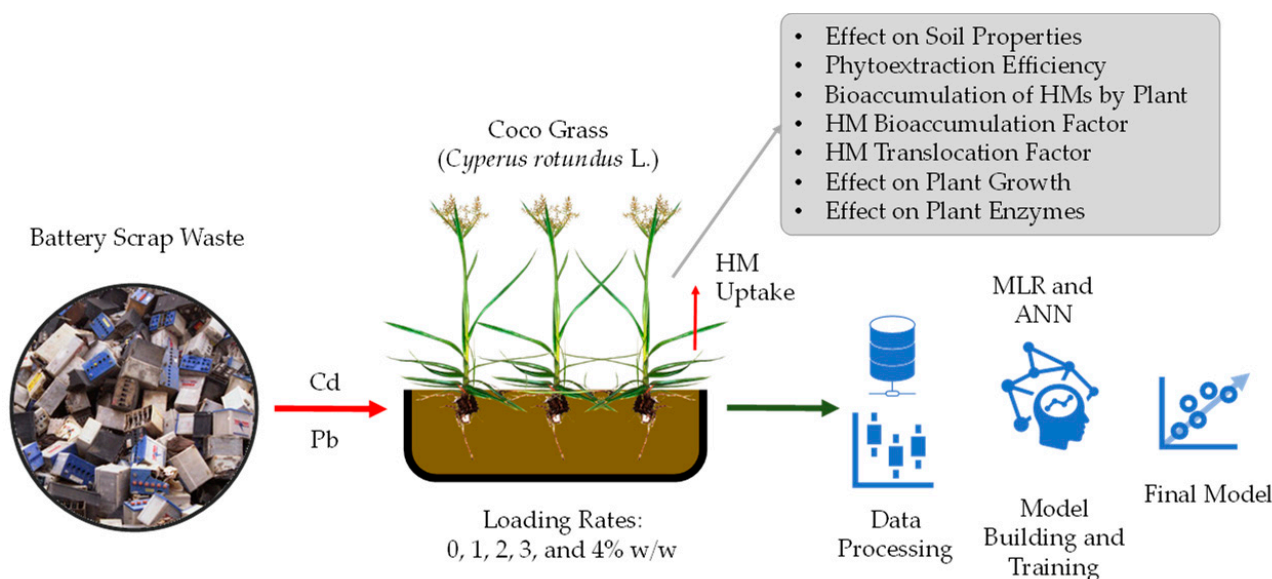


Figure 1. Experimental design for phytoextraction of Cd and Pb from soils contaminated with battery scrap waste using coco grass (*C. rotundus*).

2.3. Analytical and Instrumental Methods

The arable soil used in this study was analyzed before and after BSW mixing, as well as after phytoextraction experiments. Purposely, the pH of the soil was analyzed using a microprocessor-based digital meter (1611, ESICO International, Parwanoo, India). Cation exchange capacity (CEC) was measured as previously outlined by Kriti et al. [33]. Organic matter (OM) of soil was determined using Walkley and Black method [34]. Redox potential (mV) was measured using a meter. The texture of the soil was determined based on the percent composition of clay, silt, and sand content as previously outlined by Bharti et al. [35]. On the other hand, the contents of cadmium (Cd) and lead (Pb) in experimental soil and *C. rotundus* parts (shoot and root) were determined based on inductively coupled plasma optical emission spectroscopy (ICP-OES: 7300 DV, Perkin Elmer, Waltham, MA, USA). For this, total and bioavailable Cd and Pb contents were determined by two different extraction methods, i.e., di-acid and ethylenediaminetetraacetic acid (EDTA)-based digestion, respectively. For total metal content, a di-acid extraction solution with a 1:3 ratio containing HClO₄ and HNO₃ was used to digest soil samples at 180 °C for 2 h. For bioavailable heavy metal extraction, a 0.05 M EDTA solution was used to digest samples for 12 h on a mechanical shaker at room temperature [36]. The instrument was calibrated as per the manufacturer's instructions using standard reference materials. The detection limits of ICP-OES for Cd and Pb determination were 0.01 and 0.10 ppb, respectively. Appropriate quality control measures, such as replicate analysis, cross-validation, and certified reference materials, were ensured for the accuracy and precision of the results.

2.4. Data Analysis

In this study, the Cd and Pb removal efficiency and removal rate of *C. rotundus* grown on BSW-amended soils were computed using the following Equations (1) and (2):

$$\text{Removal efficiency (\%)} = [(HM_i - HM_f)/HM_i] \times 100 \quad (1)$$

$$\text{Removal Rate (mg}\cdot\text{kg}^{-1}\text{day}^{-1}) = HMP/t \quad (2)$$

where HM_i and HM_f refer to initial and final HM concentrations in arable soil (before and after experiments), while HMP indicates heavy metal concentration in *C. rotundus* after t

time (45 days). The Cd and Pb uptake potential of *C. rotundus* was computed using the bioaccumulation factor (BAF) index [37] as given in the following Equation (3):

$$\text{Bioaccumulation factor (BAF)} = \text{HMp}/\text{HMs} \quad (3)$$

where, HMp and HMs denote the ratio of HM concentration in plant and experimental soil, respectively. The ability of *C. rotundus* to mobilize HM from its root region to shoot was calculated using the translocation factor [38] as per the following Equation (4):

$$\text{Translocation factor (Tf)} = \text{HMsh}/\text{HMro} \quad (4)$$

where, HMsh and HMro refer to the HM concentration in the shoot and root parts of *C. rotundus*, respectively.

Two different modeling approaches, i.e., multiple linear regression (MLR) and artificial neural network (ANN), were adopted to predict the amount of Cd and Pb accumulated by *C. rotundus*. Both MLR and ANN have widely accepted tools for monitoring HM in phytoextraction experiments [39,40]. MLR establishes a linear relationship between the input and output factors. In this study, the selected soil properties, such as pH, CEC, OM, and HM concentration, were taken as input (independent) variables while the total amount of heavy metal accumulated by *C. rotundus* was considered an output (dependent) variable. The following MLR function (Equation (5)) was used to compute the Cd and Pb uptake amount (y : $\text{mg}\cdot\text{kg}^{-1}$):

$$y = a + (b \times \text{pH}) + (c \times \text{CEC}) + (d \times \text{OM}) + (e \times \text{HMs}) \quad (5)$$

Here, a is the regression intercept, while b , c , d , and e are the regression coefficients for pH, CEC, OM, and HMs as independent variables, respectively.

On the other hand, the ANN approach was also used to predict HM uptake by *C. rotundus*. For this purpose, a neural network was created comprising three different processing layers, i.e., input, hidden, and output layers. For this, the input layer is comprised of four nodes or neurons ($n = 4$) referring to the same independent variables as in the case of the MLR model. The hidden layer had ten neurons ($n = 10$) while the output layer had only one neuron ($n = 1$), indicating the predicted response (y) in terms of effective HM uptake by *C. rotundus*. A widely used logistic model activation function was used for model training. This is a sigmoid-type function that can take in any number of inputs (x) and constrain the output to be between 0 and 1 [41]. The form of the model is given in Equation (6):

$$f(x) = 1/(1 + \exp(-x)) \quad (6)$$

The whole dataset was categorized into three groups (training: 70%; testing: 15%; and validation: 15%). The learning rate of the model was adjusted to 0.001 with maximum iterations of 10,000 and epochs of 100. Figure 2 shows the overall architecture of the proposed ANN with different numbers of input/output layers and their respective neurons. Using specific validation tools, such as measured vs. predicted response values, coefficient of determination (R^2), Nash–Sutcliffe model efficiency (ME) coefficient, and root mean square error (RMSE), the created MLR and ANN models were evaluated for the goodness of fit and accuracy [42]. The following Equations (7)–(9) were used for the computation of R^2 , ME, and RMSE:

$$R^2 = 1 - \frac{\sum_{i=1}^n (y_{\text{obs}} - y_{\text{pre}})^2}{\sum_{i=1}^n (y_{\text{obs}} - \bar{y}_{\text{mean}})^2} \quad (7)$$

$$\text{ME} = 1 - \frac{\sum_{i=1}^n (y_{\text{obs}} - y_{\text{pre}})^2}{\sum_{i=1}^n (y_{\text{obs}} - \bar{y}_{\text{mean}})^2} \quad (8)$$

$$\text{RMSE} = \sqrt{\frac{\sum_{i=1}^n (y_{\text{obs}} - y_{\text{pre}})^2}{n}} \quad (9)$$

where, y_{obs} , y_{pre} , and y_{mean} are experimental, predicted, and mean values of HM content in *C. rotundus*.

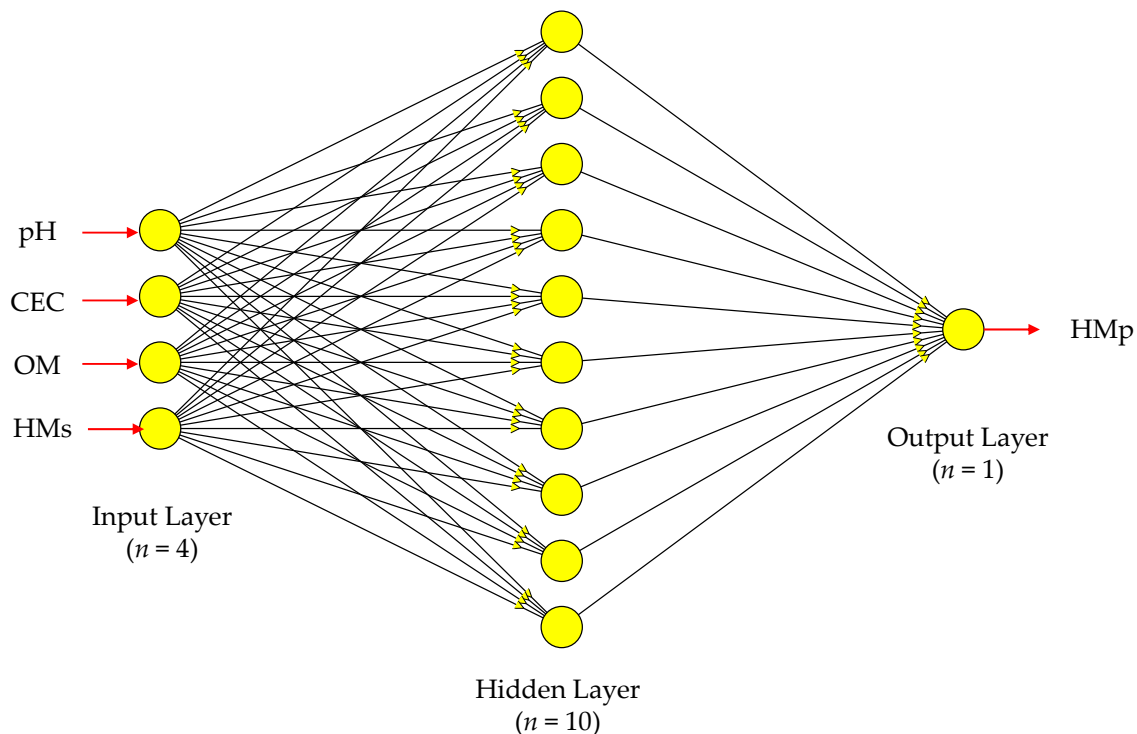


Figure 2. Design of the artificial neural network depicting different neurons and layers (Shi et al. 2023).

2.5. Software and Statistics

All experiments were performed in triplicate ($n = 3$). The data obtained in this study were analyzed using Pearson correlation and Tukey's post-hoc test to understand the significant impacts of BSW mixing on the soil as well as on *C. rotundus* properties. The level of statistical significance was $p < 0.05$. The data were analyzed using OriginPro (Version 2023, OriginLab Corp., Northampton, MA, USA) and the "nntool" function of MATLAB (Version 2021, MathWorks, Natick, MA, USA) software packages.

3. Results and Discussion

3.1. Impact of Battery Waste on Soil Properties and Cd-Pb Bioavailability

Table 1 depicts the impact of BSW mixing on the physicochemical and heavy metal properties of soil used for the cultivation of *C. rotundus*. The results show that BSW mixing had a significant ($p < 0.05$) impact on selected soil properties. In particular, it was observed that the initial pH (7.23) of arable soil was significantly ($p < 0.05$) increased after BSW mixing in different ratios, i.e., 7.55–8.35. This increase was for different BSW treatments, including T1, T2, T3, and T4 as follows: 4.42, 5.53, 9.40, and 15.49%, respectively. The increase in soil pH might be associated with the mixing of electrolytes (usually 30% NaOH) present in several Ni-Cd batteries. However, Pb-acid batteries also contain H_2SO_4 , which might decrease the pH of soil [33]. Instead, the increased pH might be due to a larger proportion of Ni-Cd batteries in the BSW used in this study. Likewise, the CEC of soil was significantly ($p < 0.05$) increased by 5.13, 7.45, 8.92, and 10.51% in different BSW treatments, such as T1, T2, T3, and T4, respectively. The ability to retain and exchange ions is influenced by basic conditions, which can alter soil CEC [43]. However, the content of OM was drastically reduced after BSW addition from 2.27 to 2.19, 2.11, 2.05, and 1.86% for T1, T2, T3, and T4 BSW treatments, correspondingly. This might be due to the addition of BSW with no OM, which reduced OM proportion in the experimental soil. Similarly, the redox potential of soil

was also significantly ($p < 0.05$) reduced after the BSW amendment, i.e., from 318.84 mV in control to 89 mV in T4. The reduction in redox potential was less in the T1 treatment (9.37%) while it reached maximum in the T4 treatment (256.75%). Herein, the mixing of BSW could result in the release of certain reducing chemical species in the soil, which could deplete the oxygen levels, thereby reducing redox potential [33].

Table 1. Effect of battery scrap waste (BSW) on physicochemical and heavy metal properties of experimental soil.

Properties	Experimental Treatments				
	Control	T1: 1% BSW	T2: 2% BSW	T3: 3% BSW	T4: 4% BSW
pH	7.23 ± 0.04 ^a	7.55 ± 0.03 ^b	7.63 ± 0.07 ^b	7.91 ± 0.05 ^c	8.35 ± 0.10 ^d
CEC (cmol·kg ⁻¹)	8.18 ± 0.09 ^a	8.60 ± 0.12 ^b	8.79 ± 0.06 ^b	8.91 ± 0.09 ^{bc}	9.04 ± 0.03 ^c
Organic matter (%)	2.27 ± 0.03 ^a	2.19 ± 0.02 ^b	2.11 ± 0.04 ^c	2.05 ± 0.03 ^c	1.86 ± 0.06 ^d
Redox potential (mV)	318.84 ± 4.10 ^a	291.50 ± 9.81 ^b	210.73 ± 6.30 ^c	163.15 ± 10.21 ^d	89.37 ± 7.58 ^e
Clay (%)	19.20 ± 1.80	-	-	-	-
Silt (%)	42.10 ± 2.90	-	-	-	-
Sand (%)	38.60 ± 1.40	-	-	-	-
Total Cd (mg·kg ⁻¹) *	0.04 ± 0.01 ^a	40.48 ± 0.52 ^b	75.20 ± 2.06 ^c	117.36 ± 7.10 ^d	152.02 ± 4.75 ^e
Total Pb (mg·kg ⁻¹) *	0.06 ± 0.01 ^a	110.06 ± 6.84 ^b	217.91 ± 10.38 ^c	340.40 ± 15.24	470.15 ± 12.62 ^e
Bioavailable Cd (mg·kg ⁻¹)	0.00 ± 0.00 ^a	11.26 ± 0.30 ^b	24.50 ± 1.05 ^c	38.17 ± 2.18 ^d	49.40 ± 3.85 ^d
Bioavailable Pb (mg·kg ⁻¹)	0.01 ± 0.00 ^a	32.50 ± 0.85 ^b	84.21 ± 5.30 ^c	107.82 ± 9.46 ^d	152.24 ± 14.67 ^e

Values are mean ± SD of three replicates ($n = 3$); CEC: cation exchange capacity; the same letters (a–e) indicate no significant difference among treatment groups at $p < 0.05$; *: threshold value (Cd: 0.80 mg·kg⁻¹ and Pb: 85 mg·kg⁻¹) in the soil as recommended by WHO (1996).

On the other hand, the total and bioavailable concentrations of selected HMs, i.e., Cd and Pb, were significantly ($p < 0.05$) increased after BSW treatment. BSW are generally rich in metallic and electrolyte wastes, which could be the source of Cd and Pb. Cd and Pb metals are primarily cast-off in the manufacturing of Ni-Cd and Pb-acid batteries, which are commonly used for wireless communication devices, while Pb-acid batteries are used in automobiles, solar plates, inverters, power backup systems, etc. The levels of Cd and Pb were considerably higher in BSW-treated soil as suggested by the threshold limits of the WHO [44]. The impact of different types of battery waste has been previously outlined by other authors [45–47]. Among them, Chowdhury et al. [45], investigated the impact of Pb-acid battery waste on the soil properties in a residential community in Bangladesh. They reported that Pb concentration in soil ranged between 94 and 119,000 mg·kg⁻¹ against the threshold value of 80.00 mg·kg⁻¹. Similarly, Ogundiran et al. [46] also studied the soil properties of abandoned Pb-acid battery dumpsite and found that the concentration of Pb and Cd reached >25,900 and 3.3 mg·kg⁻¹ maximally up to a depth of 0–15 cm. Another study by Orjiakor et al. [47] found that automobile batter waste contamination significantly ($p < 0.01$) induced the soil physicochemical properties and elevated levels of Pb, Zn, Cd, Cr, and Cu HMs compared with those in non-affected soils. Therefore, the results of these reports are in accordance with those obtained in the present study.

3.2. Cd and Pb Removal by Coco Grass (*C. rotundus*)

In this study, *C. rotundus* demonstrated a significant ability to remove Cd and Pb contents from BSW-contaminated soils. In particular, the contents of Cd and Pb significantly ($p < 0.05$) declined after 45 days of phytoextraction experiments (Table 2). Although the contents of both Cd and Pb removed were higher in a higher dose of BSW mixing, the removal efficiency was reported to decline with an increase in BSW dose from 1 to 4%. The values of removal efficiency for control, T1, T2, T3, and T4 treatments accounted for 75, 35, 44, 31, and 26% for Cd, while the values for Pb were 83, 48, 40, 29, and 22%, respectively. The average Cd and Pb removal rates were found to be increasing with an increase in BSW dose. However, removal rates of both Cd and Pb were more identical in

T3 and T4 treatments, which indicates that the plant may have reached saturation level for BSW loading.

Table 2. Changes in the soil Cd and Pb concentration before and after phytoextraction using coco grass (*C. rotundus*) grown in soils amended with battery scrap waste (BSW).

Heavy Metal	Variable	Experimental Treatments				
		Control	T1: 1% BSW	T2: 2% BSW	T3: 3% BSW	T4: 4% BSW
Cd	Initial concentration (mg·kg ⁻¹)	0.04 ± 0.01 ^a	40.48 ± 0.52 ^a	75.20 ± 2.06 ^a	117.36 ± 7.10 ^a	152.02 ± 4.75 ^a
	Final concentration (mg·kg ⁻¹)	0.01 ± 0.00 ^b	25.98 ± 1.75 ^b	42.08 ± 3.63 ^b	80.40 ± 4.60 ^b	112.30 ± 6.14 ^b
	Removal efficiency (%)	75	35	44	31	26
	Removal rate (mg·kg ⁻¹ day ⁻¹)	0.001	0.242	0.552	0.616	0.662
Pb	Initial concentration (mg·kg ⁻¹)	0.06 ± 0.01 ^a	110.06 ± 6.84 ^a	217.91 ± 10.38 ^a	340.40 ± 15.24 ^a	470.15 ± 12.62 ^a
	Final concentration (mg·kg ⁻¹)	0.01 ± 0.00 ^b	56.26 ± 2.70 ^b	130.50 ± 7.41 ^b	240.00 ± 10.65 ^b	365.09 ± 18.34 ^b
	Removal efficiency (%)	83	48	40	29	22
	Removal rate (mg·kg ⁻¹ day ⁻¹)	0.001	0.897	1.457	1.673	1.751

Values are mean ± SD of three replicates ($n = 3$); the same letters (a, b) indicate no significant difference between initial and final concentration values at $p < 0.05$.

Recent studies have demonstrated the capability of *C. rotundus* to eradicate different hazardous heavy metals [48]. Garba et al. [49] reported that *C. rotundus* can tolerate Cd, Pb, Zn, and Ni stress of up to 1000 mg·kg⁻¹. Another study by Bordoloi and Basumatary [50] showed that *C. rotundus* significantly removed Pb (43.8%), Mn (27%), and Cd (31%) metals from soils contaminated with crude soil. Similarly, Jahan-Nejati et al. [51] studied the Cu removal performance of *C. rotundus* under different mixing rates (0–300 mg·kg⁻¹) in pod soil. They observed the quadratic model showing good fitness and optimum rate for Cu removal over time. Likewise, Tripathy et al. [52] studied the impact of pulp and paper mill effluent on Hg and Cd accumulation in *C. rotundus*. They reported that *C. rotundus* had a high potential to remove Hg and Cd from pulp and paper mill effluent-contaminated sites. These reports outlined that *C. rotundus* is considered a good phytoextraction candidate for the removal of hazardous HMs from contaminated sites [50], which is also supported by the results obtained in the current study. Therefore, our study also confirmed that Cd and Pb were efficiently removed by *C. rotundus* from BSW-mixed soil.

3.3. Cd and Pb Bioaccumulation Efficiency of Coco Grass (*C. rotundus*)

Phytoremediation plants have evolved to grow in hostile soil environments. Such plants can lower HM stress in their rhizosphere by accumulating them in their vegetative parts, thereby contributing to soil decontamination [53]. This feature makes them ideal candidates for soil remediation using green technology. In the present investigation, it was observed that *C. rotundus* significantly ($p < 0.05$) accumulated the contents of Cd and Pb from BSW-contaminated soils (Table 3). However, root parts of *C. rotundus* showed higher Cd and Pb bioaccumulation compared with the shoot and whole plant body. The overall order of Cd and Pb bioaccumulation by *C. rotundus* was observed as root > whole plant > shoot. When compared with the control treatment, the levels of Cd and Pb in *C. rotundus* tissues increased with an increase in the BSW mixing dose. However, there was a much less significant difference between the T3 and T4 treatments, which might be because the plant already achieved its saturation point in the 3% BSW treatment. The highest concentrations of Cd and Pb were encountered in root parts of *C. rotundus* for T4 treatment, i.e., 38.81 and 109.06 mg·kg⁻¹, respectively.

Table 3. Bioaccumulation and translocation of Cd and Pb by phytoextraction using coco grass (*C. rotundus*) grown in soils amended with battery scrap waste (BSW).

Heavy Metals	Experimental Treatments	Concentration (mg·kg ⁻¹ dwt.)			Bioaccumulation Factor (Soil → Plant)			Translocation Factor (Root → Shoot)
		Shoot	Root	Whole Plant	Shoot	Root	Whole Plant	
Cd	Control	0.01 ± 0.00 ^a	0.03 ± 0.01 ^a	0.02 ± 0.01 ^a	0.25	0.75	0.50	0.33
	T1: 1% BSW	4.90 ± 0.13 ^b	12.50 ± 0.28 ^b	9.67 ± 0.19 ^b	0.12	0.31	0.24	0.39
	T2: 2% BSW	13.04 ± 0.50 ^c	30.10 ± 1.07 ^c	22.08 ± 0.65 ^c	0.17	0.40	0.29	0.43
	T3: 3% BSW	17.62 ± 1.17 ^d	37.90 ± 2.24 ^d	24.64 ± 1.72 ^{cd}	0.15	0.32	0.21	0.46
	T4: 4% BSW	21.30 ± 0.92 ^e	38.81 ± 1.59 ^d	27.43 ± 1.24 ^d	0.14	0.26	0.18	0.55
Pb	Control	0.01 ± 0.01 ^a	0.04 ± 0.01 ^a	0.03 ± 0.01 ^a	0.17	0.67	0.50	0.25
	T1: 1% BSW	7.13 ± 0.20 ^b	30.85 ± 1.34 ^b	21.62 ± 0.90 ^b	0.06	0.28	0.20	0.23
	T2: 2% BSW	16.04 ± 0.61 ^c	87.40 ± 7.95 ^c	55.17 ± 4.34 ^c	0.07	0.40	0.25	0.18
	T3: 3% BSW	19.32 ± 0.49 ^d	103.27 ± 4.01 ^d	69.01 ± 9.42 ^{cd}	0.06	0.30	0.20	0.19
	T4: 4% BSW	22.65 ± 1.80 ^{de}	109.06 ± 6.27 ^d	76.10 ± 6.05 ^d	0.05	0.23	0.16	0.21

Values are mean ± SD of three replicates ($n = 3$); the same letters (a–e) indicate no significant difference among treatment groups at $p < 0.05$.

Long-term monitoring of BAF in polluted soils is helpful in understanding the effectiveness of phytoremediation over time and setting up regulatory compliances for the same. BAF also helps in determining the frequency of HMs migration to upper trophic levels within the food chain. The highest BAF values were reported for root parts, which were subjected to the highest bioaccumulation amount. However, BAF decreased with an increase in BSW dose, which was largely associated with concentration-induced toxicity in soil medium. Similarly, the Tf analysis showed that the migration of Cd and Pb from root to shoot parts of *C. rotundus* was significantly associated with the BSW mixing rate. The Tf values of Cd and Pb increased with an increase in their bioavailable concentration in the soil. Herein, the highest Tf values reported for Cd and Pb were 0.55 and 0.25, respectively. Nevertheless, the Tf values for Cd were positively associated with BSW dose while those for Pb had negative associations. The Pearson correlation matrix given in Figure 3 shows that selected soil parameters (pH, CEC, OM, RP, and HMs) were significantly ($p < 0.05$) correlated with the HMs bioaccumulation by *C. rotundus*. In general, pH was negatively correlated with OM ($r = -0.99$) and RP ($r = -0.97$) of experimental soil. However, the BSW mixing rate showed a significant negative influence on soil OM and RP. The contents of HMs in both soil and *C. rotundus* were negatively correlated. Herein, all other soil parameters showed a significant positive correlation with soil and plant HM contents.

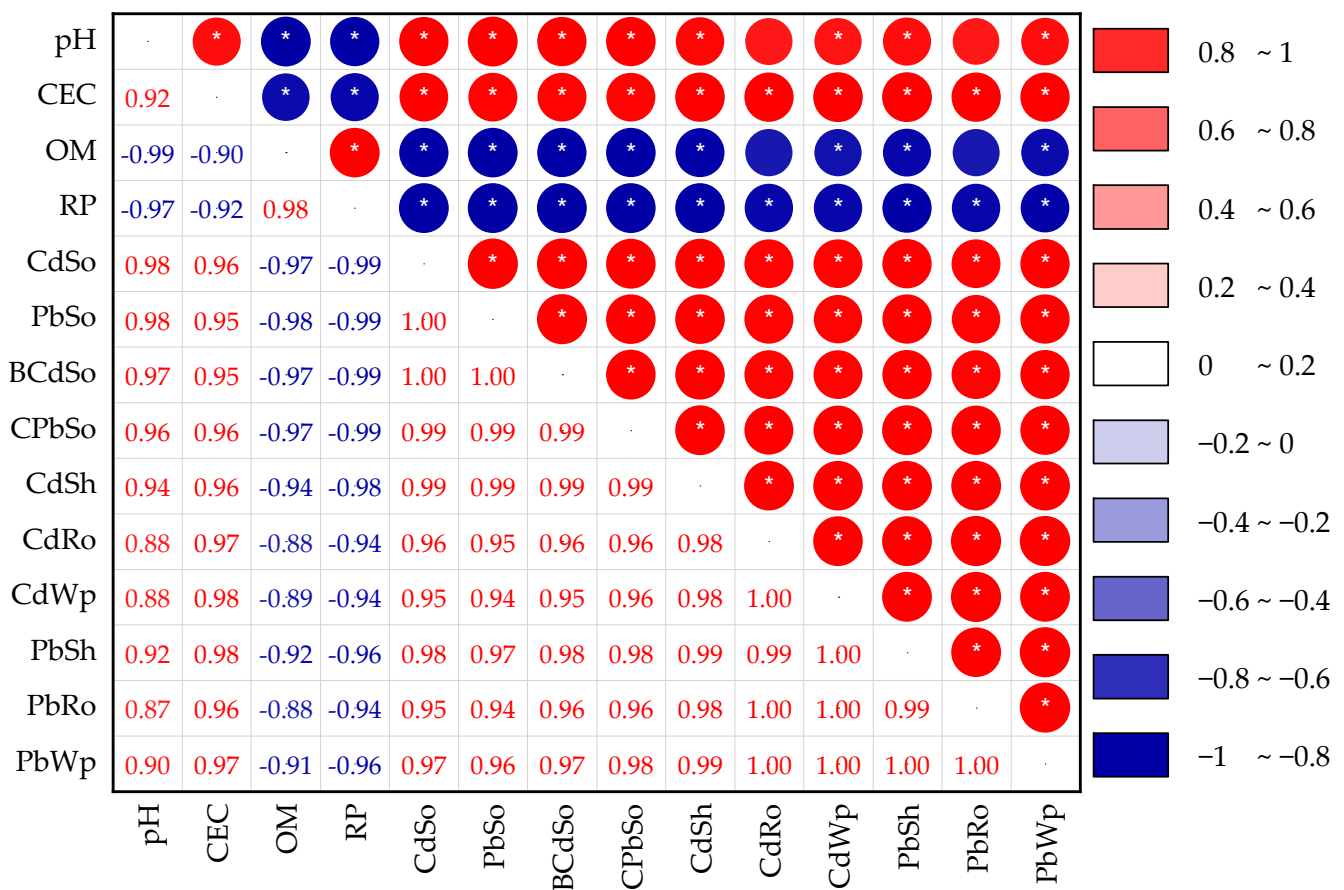


Figure 3. Pearson correlation matrix for interaction between soil properties and heavy metal uptake by coco grass (*C. rotundus*) grown in soils amended with battery scrap waste (BSW) (CEC: cation exchange capacity; OM: organic matter; RP: redox potential; CdSo: Cd in soil; PbSo: Pb in soil; CdSh: Cd in the shoot; CdRo: Cd in the root CdWp: Cd in the whole plant; PbSh: Pb in the shoot; PbRo: Pb in the root; and PbWp: Pb in the whole plant; *: significant at $p < 0.05$).

Bioaccumulation of several HMs by *C. rotundus* has been previously reported in several studies [10,54–56]. In particular, Khandare et al. [54] investigated the bioaccumulation and translocation of fluoride (F) by *C. rotundus*. They found that *C. rotundus* showed good potential for accumulating F contents within leaf and root parts where the highest BAF and Tf were 1.07 and 0.52, respectively. Halder et al. [55] also found that *C. rotundus* accumulated $>350 \text{ mg}\cdot\text{kg}^{-1}$ of Pb in roots while only $<50 \text{ mg}\cdot\text{kg}^{-1}$ in shoot parts accounting for BAF values of >20 , respectively. Moreover, Nwaichi et al. [32] reported that *C. rotundus* accumulated significant contents of Pb (0.18), Cr (0.60), Cd (0.01), and Ni (0.1) from crude oil-contaminated soils. Similarly, Khan [56] observed HMs bioaccumulation by *C. rotundus* growing near the riparian zone of Lahat, Malaysia. ICP-MS analysis revealed that root parts of *C. rotundus* had the highest HM concentration with maximum BAF and Tf values, which is in line with those observed in the current study.

3.4. Effect of Battery Waste on Growth, Biochemical, and Enzyme Response of *C. rotundus*

Since HM stress may result in inefficient growth and physiological mechanisms, it is essential to monitor the biochemical response to ensure the suitability of plants in phytoextraction. Table 4 shows the effect of BSW amendment on the growth, biochemical, and enzyme response of *C. rotundus* in this study. It was observed that BSW application significantly ($p < 0.05$) reduced the plant's growth and biochemical parameters. Specifically, control and T1 showed a non-significant ($p > 0.05$) difference for the change in plant height and weight, and root length; however, these were significantly ($p < 0.05$) higher in the rest of the treatments, i.e., T2, T3, and T4. The maximum average plant height (34.27 cm), fresh weight (6.35 g), dry weight (1.80 g), root length (8.56 cm), and relative growth rate ($0.14 \text{ g}\cdot\text{day}^{-1}$) were found in the control treatment whereas the minimum was observed in the T4.

Table 4. Impact of Cd and Pb on plant growth, biochemical, and enzyme activity responses of coco grass (*C. rotundus*) grown in soils amended with battery scrap waste (BSW).

Parameters	Experimental Treatments				
	Control	T1: 1% BSW	T2: 2% BSW	T3: 3% BSW	T4: 4% BSW
Plant height (cm)	34.27 ± 2.50 ^c	32.30 ± 1.74 ^c	27.93 ± 1.25 ^b	24.68 ± 2.40 ^{ab}	21.01 ± 1.18 ^a
Fresh weight (g·plant ⁻¹)	6.35 ± 0.04 ^e	5.84 ± 0.09 ^d	4.16 ± 0.13 ^c	3.95 ± 0.05 ^b	3.60 ± 0.10 ^a
Dry weight (g·plant ⁻¹)	1.80 ± 0.04 ^{de}	1.71 ± 0.07 ^d	1.40 ± 0.06 ^c	1.16 ± 0.12 ^{ab}	1.09 ± 0.05 ^a
Root length (g)	8.56 ± 0.12 ^{de}	8.20 ± 0.15 ^d	7.58 ± 0.09 ^c	7.10 ± 0.22 ^b	6.74 ± 0.08 ^a
Relative growth rate (g·day ⁻¹)	0.14	0.13	0.09	0.09	0.08
Chlorophyll content (mg·g ⁻¹ fwt.)	2.42 ± 0.04 ^e	2.31 ± 0.02 ^d	2.05 ± 0.03 ^c	1.92 ± 0.06 ^b	1.80 ± 0.04 ^a
Carotenoids (mg·g ⁻¹ fwt.)	3.78 ± 0.05 ^e	3.60 ± 0.09 ^d	3.11 ± 0.10 ^{bc}	2.80 ± 0.13 ^b	2.56 ± 0.07 ^a
Tuber carbohydrates (%)	24.98 ± 1.18 ^{cd}	22.10 ± 1.70 ^{bc}	19.66 ± 0.91 ^b	16.05 ± 1.58 ^a	15.93 ± 2.20 ^a
Superoxide dismutase (U·mg ⁻¹ P)	2.60 ± 0.08 ^a	3.51 ± 0.14 ^b	5.73 ± 0.32 ^c	6.04 ± 0.21 ^{cd}	8.25 ± 0.74 ^e
Catalase (μmol·min ⁻¹ mg ⁻¹ P)	1.70 ± 0.09 ^a	2.25 ± 0.13 ^b	3.19 ± 0.06 ^c	4.01 ± 0.02 ^d	4.10 ± 0.04 ^e
Ascorbate peroxidase (mM·mg ⁻¹ P)	3.04 ± 0.02 ^a	5.20 ± 0.10 ^b	7.58 ± 0.07 ^c	11.82 ± 0.40 ^d	12.09 ± 1.15 ^d

Values are mean ± SD of three replicates ($n = 3$); the same letters (a–e) indicate no significant difference among treatment groups at $p < 0.05$.

A sharp decline in growth parameters of *C. rotundus* might be due to the high Cd and Pb toxicity of soil that came from BSW. Moreover, the biochemical parameters of *C. rotundus*, such as chlorophyll content ($2.42 \text{ mg}\cdot\text{g}^{-1}$), carotenoids ($3.78 \text{ mg}\cdot\text{g}^{-1}$), and tuber carbohydrate (24.98%), were also reduced in all BSW treatments. As an important cell constituent, chlorophyll biosynthesis is negatively affected by the presence of hazardous HMs [57]. Similarly, carotenoids play an important role as photoprotectors and antioxidants in plant cells [58]. Reduction in carotenoids may result in several cellular deficiencies, including inefficient cell defense and lowering of photosynthesis rates [59]. The contents of carbohydrates were also reduced from 24.98 to 15.93, which is an indication of inefficient plant growth and failed photosynthesis. This is supported by the findings of present

experiments, which depict a nearly two-fold reduction in both chlorophyll and carotenoids of *C. rotundus*.

SOD acts as an important enzyme to combat oxidative defense in plant systems by the dismutation of superoxide radicals [60]. SOD levels may be elevated if plants are exposed to oxidative conditions, which helps in converting the harmful radicals to H₂O₂ [61]. BSW amendment in the current study could have resulted in an increased number of reactive oxidizing species, which is detrimental to plants. For this, SOD levels were inclined from 2.60 to 8.25 U·mg⁻¹ P (i.e., 217.30%) in control to T4 treatment, indicating that *C. rotundus* showed the ability to neutralize the oxidative stress caused by Cd and Pb. Similarly, CAT works after SOD by converting the H₂O₂ molecules to H₂O and O₂ molecules, thus accomplishing a complete defense against oxidative stress [62]. Excess H₂O₂ accumulation in plant cells could result in significant cell injuries. The elevated H₂O₂ levels are neutralized by CAT activity, which was observed in the current study where CAT levels significantly increased from 1.70 to 4.10 μmol·min⁻¹mg⁻¹ P with an increase in BSW treatment dose. Similarly, ascorbate peroxidase also breaks down excess H₂O₂ by utilizing ascorbate (vitamin C) molecules [63]. The levels of ascorbate peroxidase were significantly increased from 2.04 to 122.09 mM·mg⁻¹ P. However, the magnitude of these specific responses to upregulate stress caused by Cd and Pb may vary according to the BSW mixing rate, exposure, duration, and plant species. The Pearson correlation matrix in Figure 4 shows that soil properties had a significant impact on the growth, biochemical, and enzymatic response of *C. rotundus*.

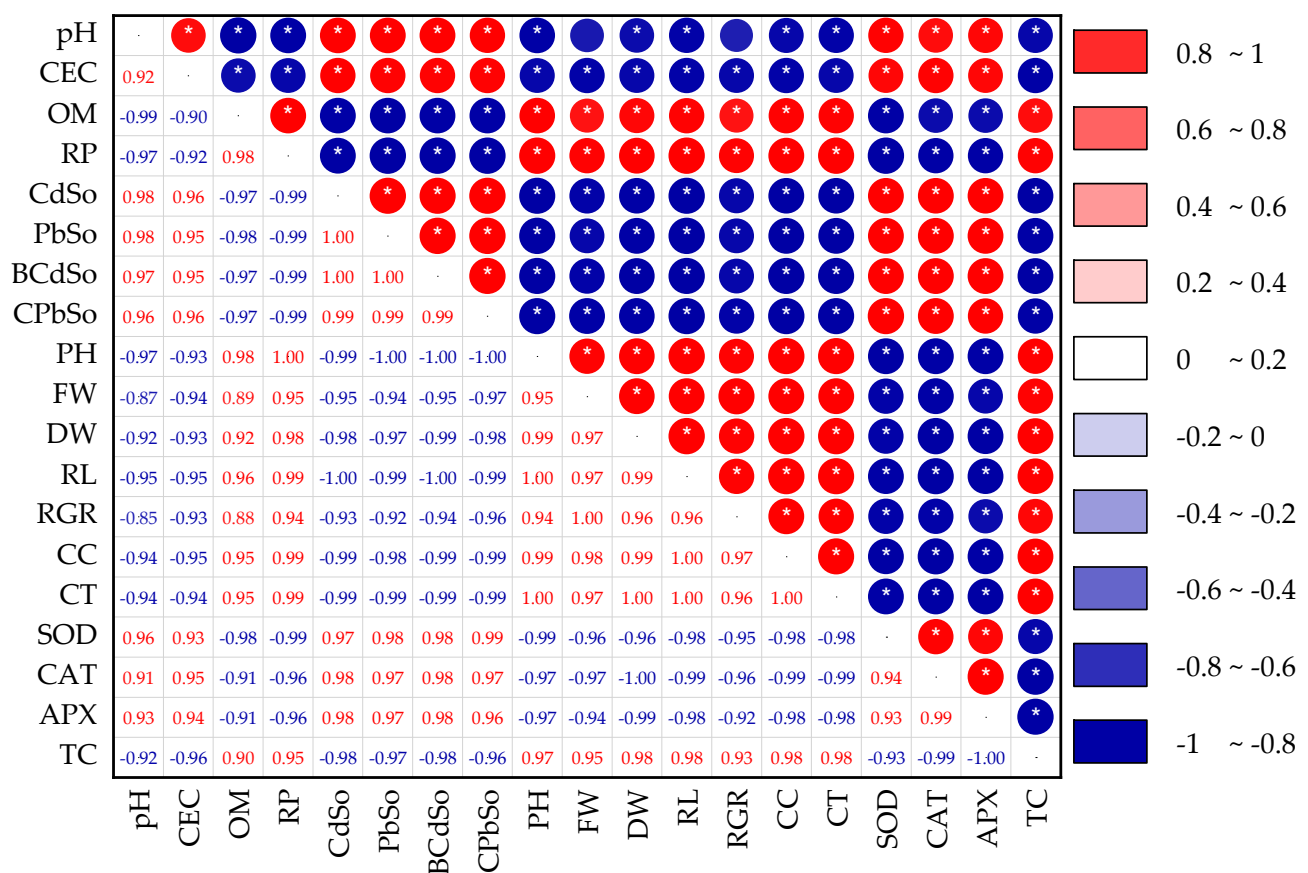


Figure 4. Pearson correlation matrix for interaction between soil properties, growth, and the enzymatic response of coco grass (*C. rotundus*) grown in soils amended with battery scrap waste (BSW) (CEC: cation exchange capacity; OM: organic matter; RP: redox potential; CdSo: Cd in soil; PbSo: Pb in soil; PH: plant height; FW: fresh weight; DW: dry weight; RL: root length; RGR: relative growth rate; CC: chlorophyll content; CT: carotenoids; SOD: superoxide dismutase; CAT: catalase; APX: ascorbate peroxidase; and TC: tuber carbohydrates; *: significant at $p < 0.05$).

The impact of hazardous HMs on plant growth, and biochemical, and enzymatic responses has been widely investigated by several authors [33,64]. Kriti et al. [33] studied the impact of Ni and Cd-rich battery waste on the physiological and enzyme response of two plants: vetiver (*Chrysopogon zizanioides* L.) and lemongrass (*Cymbopogon citratus* DC. Stapf) and found that Ni and Cd levels in the soil had significant detrimental effects on SOD, chlorophyll, carotenoid, and ascorbate peroxidase of both plants. Similarly, Adejumo et al. [64] reported that the bachelor's button (*Gomphrena celosoides* Mart.) plant showed a significant decline in soils contaminated with Pb and Cr from battery waste dumpsites in Nigeria. Overall, the results of the present study show that high Cd and Pb contents in soil could bring harmful effects on the growth and biochemical and enzymatic response of *C. rotundus* grown in BSW-contaminated soil.

3.5. Predictive Models for Cd and Pb Uptake by *C. rotundus*

The uptake of HMs by plants can be influenced by several factors, such as soil properties (pH, OM, HM's availability), type of plant, and environmental conditions. MLR and ANN are widely used to construct predictive relationships between these parameters and the amount of HMs absorbed by phytoremediation plants [65]. In this study, it was observed that both MLR and ANN models showed good fitness to predict the uptake of Cd and Pb by *C. rotundus* tissues. Table 5 shows the developed MLR- and ANN-based prediction models and their validation parameters. For MLR, the models showed good coefficient of determination (R^2) values ranging from 0.98 to 0.99. Herein, pH showed a negative coefficient for both HMs uptake by shoot, root, and whole plant parts of *C. rotundus*, while other independent variables (CEC, OM, and HMs) had positive coefficient values. The ME values of MLR models ranged between 0.98 and 0.99, while RMSE was recorded >5.72 , indicating that the developed equations can predict HMs uptake with high efficiency and low error. On the other hand, ANN showed slightly better R^2 values (0.99) for all models. The ME and RMSE values were recorded as 0.99 and >0.84 , respectively, which indicates better goodness of fit. As depicted in Figure 5, the experimental vs. model predicted scatter plot clearly shows that responses predicted by ANN models were highly close to experimental values compared with those of MLR models. This supports the fact of low prediction error.

However, MLR requires manual feature extraction in which the selection of suitable input parameters is decided based on their overall influence on the model. This problem is efficiently addressed by an ANN, which can automatically identify relevant variables from the input dataset, thereby reducing the need for manual feature extraction. Moreover, ANN models are known to have better prediction accuracy if trained using a well-curated and large number of input data points [66]. ANN algorithms can capture nonlinear relationships between input and output variables, which is generally difficult for other models, such as MLR. Although MLR is a traditional predictive technique that creates a linear function between input and output response, it is still useful for constructing mathematical models for simple and small-scale experiments and it provides valuable insight into HM uptake predictions [39].

Recent studies have employed linear and nonlinear models for the prediction of HMs uptake by plants under different phytoremediation systems [67,68]. However, only a few employed prediction modeling for BSW-based phytoremediation systems [25,33,69]. Among them, Kriti et al. [33] developed MLR and nonlinear sigmoid models for the prediction of Ni and Cd by *C. zizanioides* and *C. citratus* plants grown in soils mixed with battery electrolyte waste. They reported that MLR models were more efficient for Ni and Cd prediction compared with sigmoid models as indicated by experimental vs. predicted, R^2 (>0.88), and Nash–Sutcliffe ME (>0.87) values. Similarly, Priyadarshini et al. [25] created MLR and machine learning-based prediction models for HM's recovery from spent Zn-Mn batteries. They also confirmed that machine-learning models had better fitness compared with MLR. In their study, Bajestani et al. [69] evaluated the application of quadric regression modeling (response surface method) for optimization of Ni, Cd, and Co bio-recovery from

spent household battery waste using *Acidithiobacillus ferrooxidans*. Thus, the combination of both MLR and ANN models could provide complementary strengths to improved prediction of HMs uptake by *C. rotundus*.

Table 5. Comparative assessment of MLR and ANN predictive models for Cd and Pb uptake by coco grass (*C. rotundus*) grown in soils amended with battery scrap waste (BSW).

Model Type	Heavy Metals	Plant Parts	Model Equation	R ²	ME	RMSE
MLR	Cd	Shoot	$40.82 - 8.72 \times \text{pH} + 1.88 \times \text{CEC} + 2.89 \times \text{OM} + 0.20 \times \text{HM}_{\text{So}}$	0.99	0.99	0.67
		Root	$93.48 - 36.00 \times \text{pH} + 16.51 \times \text{CEC} + 14.05 \times \text{OM} + 0.46 \times \text{HM}_{\text{So}}$	0.99	0.99	1.34
		Whole Plant	$20.14 - 22.24 \times \text{pH} + 18.35 \times \text{CEC} - 4.06 \times \text{OM} + 0.22 \times \text{HM}_{\text{So}}$	0.98	0.98	1.43
	Pb	Shoot	$4.39 - 14.61 \times \text{pH} + 10.70 \times \text{CEC} + 6.20 \times \text{OM} + 0.06 \times \text{HM}_{\text{So}}$	0.98	0.98	1.07
		Root	$296.99 - 129.12 \times \text{pH} + 55.68 \times \text{CEC} + 80.29 \times \text{OM} + 0.50 \times \text{HM}_{\text{So}}$	0.98	0.98	5.72
		Whole Plant	$43.87 - 63.20 \times \text{pH} + 30.51 \times \text{CEC} + 72.24 \times \text{OM} + 0.31 \times \text{HM}_{\text{So}}$	0.98	0.98	3.21
ANN	Cd	Shoot	-	0.99	0.99	0.23
		Root	-	0.99	0.99	0.80
		Whole Plant	-	0.99	0.99	0.45
	Pb	Shoot	-	0.99	0.99	0.30
		Root	-	0.99	0.99	0.34
		Whole Plant	-	0.99	0.99	0.84

MLR: multiple linear regression; -: not applicable; ANN: artificial neural network; ME: model efficiency; RMSE: root mean square error.

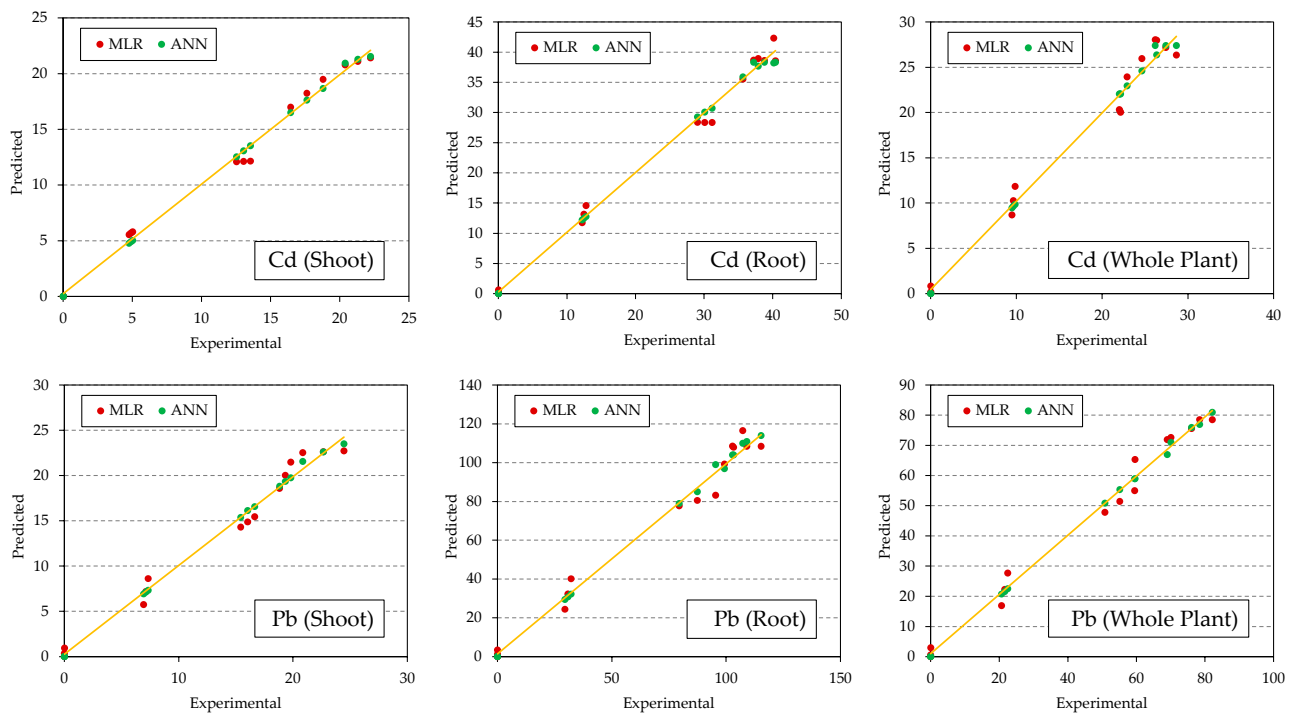


Figure 5. Experimental vs. model predicted (MLR: multiple linear regression; ANN: artificial neural network) values for Cd and Pb uptake by coco grass (*C. rotundus*) grown in soils amended with battery scrap waste (BSW).

4. Conclusions

The results revealed that BSW mixing in soil significantly elevated the levels of Cd and Pb ($p < 0.05$), which were maximally taken by *C. rotundus* into root parts. The excess uptake of Cd and Pb by *C. rotundus* resulted in reduced growth and biochemical parameters while inducing the levels of stress enzymes. The BAF and Tf values also indicated that *C. rotundus* was a Cd- and Pb-hyperaccumulator plant that can be used to clean up BSW-contaminated sites. Furthermore, prediction modeling results using MLR and ANN showed that both approaches were efficient for effective HMs uptake by *C. rotundus*. However, ANN models gave better results when tested using different validation tools. Overall, this study concluded that *C. rotundus* can be used as a potential phytoremediation plant for Cd and Pb phytoextraction from BSW-contaminated soils. Further studies on the bioaccumulation of other toxic HMs and their physiological and microscopic effects on *C. rotundus* with post-characterization of harvested biomass are highly recommended.

Author Contributions: Conceptualization, A.A.A.-H., M.A.T., P.K. (Pankaj Kumar) and E.M.E.; Methodology, A.A.A.-H., I.Š., V.K. and P.K. (Pankaj Kumar); Software, I.Š. and P.K. (Pankaj Kumar); Validation, A.A.A.-H., M.A.T., I.Š., M.G., B.A., K.S.C., P.K. (Piyush Kumar), V.K. and E.M.E.; Formal analysis, M.G., P.K. (Piyush Kumar) and P.K. (Pankaj Kumar); Investigation, M.G., P.K. (Piyush Kumar) and P.K. (Pankaj Kumar); Resources, V.K.; Data curation, I.Š., B.A. and K.S.C.; Writing—original draft, P.K. (Pankaj Kumar); Writing—review & editing, M.A.T., I.Š., M.G., B.A., K.S.C., P.K. (Piyush Kumar), V.K. and E.M.E.; Visualization, B.A. and K.S.C.; Supervision, E.M.E.; Project administration, A.A.A.-H., M.A.T. and E.M.E.; Funding acquisition, A.A.A.-H. and M.A.T. All authors have read and agreed to the published version of the manuscript.

Funding: This research was funded by Princess Nourah bint Abdulrahman University Researchers Supporting Project number (PNURSP2023R93), Princess Nourah bint Abdulrahman University, Riyadh, Saudi Arabia. This research was funded by the Deanship of Scientific Research at King Khalid University, Abha, Saudi Arabia (grant number RGP2/220/44).

Institutional Review Board Statement: Not applicable.

Data Availability Statement: Not applicable.

Acknowledgments: The authors express their gratitude to Princess Nourah bint Abdulrahman University Researchers Supporting Project number (PNURSP2023R93), Princess Nourah bint Abdulrahman University, Riyadh, Saudi Arabia. The authors extend their appreciation to the Deanship of Scientific Research at King Khalid University, Abha, Saudi Arabia, for funding this work through the Research Group Project under grant number RGP2/220/44.

Conflicts of Interest: The authors declare no conflict of interest.

References

- Schmidt-Rohr, K. How Batteries Store and Release Energy: Explaining Basic Electrochemistry. *J. Chem. Educ.* **2018**, *95*, 1801–1810. [[CrossRef](#)]
- Cho, J.; Jeong, S.; Kim, Y. Commercial and Research Battery Technologies for Electrical Energy Storage Applications. *Prog. Energy Combust. Sci.* **2015**, *48*, 84–101. [[CrossRef](#)]
- Grand View Research. *Battery Market Size, Share & Trends Analysis Report By Product (Lead Acid, Li-Ion, Nickel Metal Hydride, Ni-Cd)*; Grand View Research: San Francisco, CA, USA, 2020.
- Kala, S.; Mishra, A. Battery Recycling Opportunity and Challenges in India. *Mater. Today Proc.* **2021**, *46*, 1543–1556. [[CrossRef](#)]
- Dasila, H.; Joshi, D.; Verma, S.; Maithani, D.; Rawat, S.K.; Kumar, A.; Suyal, N.; Kumar, N.; Suyal, D.C. Hazardous Waste: Impact and Disposal Strategies. In *Advanced Microbial Techniques in Agriculture, Environment, and Health Management*; Elsevier: Amsterdam, The Netherlands, 2023; pp. 153–166. ISBN 9780323916431.
- Rarotra, S.; Sahu, S.; Kumar, P.; Kim, K.; Tsang, Y.F.; Kumar, V.; Kumar, P.; Srinivasan, M.; Veksha, A.; Lisak, G. Progress and Challenges on Battery Waste Management: A Critical Review. *ChemistrySelect* **2020**, *5*, 6182–6193. [[CrossRef](#)]
- Zeng, X.; Li, J. Spent Rechargeable Lithium Batteries in E-Waste: Composition and Its Implications. *Front. Environ. Sci. Eng.* **2014**, *8*, 792–796. [[CrossRef](#)]
- Sivaramanan, S. E-Waste Management, Disposal and Its Impacts on the Environment. *Univers. J. Environ. Res. Technol.* **2013**, *3*, 531–537.
- Tutic, A.; Novakovic, S.; Lutovac, M.; Biocanin, R.; Ketin, S.; Omerovic, N. The Heavy Metals in Agrosystems and Impact on Health and Quality of Life. *Open Access Maced. J. Med. Sci.* **2015**, *3*, 345–355. [[CrossRef](#)]

10. Singh, R.; Gautam, N.; Mishra, A.; Gupta, R. Heavy Metals and Living Systems: An Overview. *Indian J. Pharmacol.* **2011**, *43*, 246. [[CrossRef](#)]
11. Nordberg, G.F.; Fowler, B.A. *Risk Assessment for Human Metal Exposures*; Elsevier: Amsterdam, The Netherlands, 2019; ISBN 9780128042274.
12. Abdel-Rahman, G. Heavy Metals, Definition, Sources of Food Contamination, Incidence, Impacts and Remediation: A Literature Review with Recent Updates. *Egypt. J. Chem.* **2021**, *65*, 419–437. [[CrossRef](#)]
13. Collin, S.; Baskar, A.; Geevarghese, D.M.; Ali, M.N.V.S.; Bahubali, P.; Choudhary, R.; Lvov, V.; Tovar, G.I.; Senatov, F.; Koppala, S.; et al. Bioaccumulation of Lead (Pb) and Its Effects in Plants: A Review. *J. Hazard. Mater. Lett.* **2022**, *3*, 100064. [[CrossRef](#)]
14. Asare, M.O.; Száková, J.; Tlustoš, P. The Fate of Secondary Metabolites in Plants Growing on Cd-, As-, and Pb-Contaminated Soils—A Comprehensive Review. *Environ. Sci. Pollut. Res.* **2022**, *30*, 11378–11398. [[CrossRef](#)] [[PubMed](#)]
15. Kumar, S.; Rahman, M.A.; Islam, M.R.; Hashem, M.A.; Rahman, M.M. Lead and Other Elements-Based Pollution in Soil, Crops and Water near a Lead-Acid Battery Recycling Factory in Bangladesh. *Chemosphere* **2022**, *290*, 133288. [[CrossRef](#)] [[PubMed](#)]
16. Tauqeer, H.M.; Basharat, Z.; Adnan Ramzani, P.M.; Farhad, M.; Lewińska, K.; Turan, V.; Karczewska, A.; Khan, S.A.; Faran, G.; Iqbal, M. Aspergillus Niger-Mediated Release of Phosphates from Fish Bone Char Reduces Pb Phytoavailability in Pb-Acid Batteries Polluted Soil, and Accumulation in Fenugreek. *Environ. Pollut.* **2022**, *313*, 120064. [[CrossRef](#)] [[PubMed](#)]
17. Saxena, G.; Purchase, D.; Mulla, S.I.; Saratale, G.D.; Bharagava, R.N. Phytoremediation of Heavy Metal-Contaminated Sites: Eco-Environmental Concerns, Field Studies, Sustainability Issues, and Future Prospects. *Rev. Environ. Contam. Toxicol.* **2019**, *249*, 71–131.
18. Henschel, J.; Mense, M.; Harte, P.; Diehl, M.; Buchmann, J.; Kux, F.; Schlatt, L.; Karst, U.; Hensel, A.; Winter, M.; et al. Phytoremediation of Soil Contaminated with Lithium Ion Battery Active Materials—A Proof-of-Concept Study. *Recycling* **2020**, *5*, 26. [[CrossRef](#)]
19. Justin, M.Z.; Pajk, N.; Zupanc, V.; Zupančič, M. Phytoremediation of Landfill Leachate and Compost Wastewater by Irrigation of Populus and Salix: Biomass and Growth Response. *Waste Manag.* **2010**, *30*, 1032–1042. [[CrossRef](#)]
20. Chehregani, A.; Noori, M.; Yazdi, H.L. Phytoremediation of Heavy-Metal-Polluted Soils: Screening for New Accumulator Plants in Angouran Mine (Iran) and Evaluation of Removal Ability. *Ecotoxicol. Environ. Saf.* **2009**, *72*, 1349–1353. [[CrossRef](#)]
21. Siyar, R.; Doulati Ardejani, F.; Norouzi, P.; Maghsoudy, S.; Yavarzadeh, M.; Taherdangkoo, R.; Butscher, C. Phytoremediation Potential of Native Hyperaccumulator Plants Growing on Heavy Metal-Contaminated Soil of Khatunabad Copper Smelter and Refinery, Iran. *Water* **2022**, *14*, 3597. [[CrossRef](#)]
22. Manoj, S.R.; Karthik, C.; Kadirvelu, K.; Arulselvi, P.I.; Shanmugasundaram, T.; Bruno, B.; Rajkumar, M. Understanding the Molecular Mechanisms for the Enhanced Phytoremediation of Heavy Metals through Plant Growth Promoting Rhizobacteria: A Review. *J. Environ. Manag.* **2020**, *254*, 109779. [[CrossRef](#)]
23. Wang, Y.; Li, S.; Wang, X.; Xu, J.; Li, T.; Zhu, J.; Yang, R.; Wang, J.; Chang, M.; Wang, L. Biochelator Assisted Phytoremediation for Cadmium (Cd) Pollution in Paddy Field. *Sustainability* **2021**, *13*, 12170. [[CrossRef](#)]
24. Kumar, S.; Dube, K.K.; Rai, J.P.N. *Mathematical Model for Phytoremediation of Pulp and Paper Industry Wastewater*; CSIR: New Delhi, India, 2005; pp. 717–721.
25. Priyadarshini, J.; Elangovan, M.; Mahdal, M.; Jayasudha, M. Machine-Learning-Assisted Prediction of Maximum Metal Recovery from Spent Zinc–Manganese Batteries. *Processes* **2022**, *10*, 1034. [[CrossRef](#)]
26. Peerzada, A.M. Biology, Agricultural Impact, and Management of *Cyperus rotundus* L.: The World’s Most Tenacious Weed. *Acta Physiol. Plant* **2017**, *39*, 270. [[CrossRef](#)]
27. Baloch, A.H. The Biology of Balochistani Weed: *Cyperus rotundus* Linnaeus. A Review. *Pure Appl. Biol.* **2015**, *4*, 171–180. [[CrossRef](#)]
28. Stoller, E.W.; Sweet, R.D. Biology and Life Cycle of Purple and Yellow Nutsedges (*Cyperus rotundus* and *C. Esculentus*). *Weed Technol.* **1987**, *1*, 66–73. [[CrossRef](#)]
29. Peerzada, A.M.; Ali, H.H.; Naeem, M.; Latif, M.; Bukhari, A.H.; Tanveer, A. *Cyperus rotundus* L.: Traditional Uses, Phytochemistry, and Pharmacological Activities. *J. Ethnopharmacol.* **2015**, *174*, 540–560. [[CrossRef](#)] [[PubMed](#)]
30. Jain, P.K.; Das, D. Ethnopharmacological Study of *Cyperus rotundus* a Herb Used By Tribal Community As a Traditional Medicine for Treating Various Diseases. *Innov. J. Ayurvedic Sci.* **2016**, *4*, 4–6.
31. Basumatary, B.; Saikia, R.; Bordoloi, S. Phytoremediation of Crude Oil Contaminated Soil Using Nut Grass, *Cyperus rotundus*. *J. Environ. Biol.* **2012**, *33*, 891–896.
32. Nwaichi, E.O.; Chukwuere, C.O.; Abosi, P.J.; Onukwuru, G.I. Phytoremediation Of Crude Oil Impacted Soil Using Purple Nutsedge. *J. Appl. Sci. Environ. Manag.* **2021**, *25*, 475–479. [[CrossRef](#)]
33. Kriti; Basant, N.; Singh, J.; Kumari, B.; Sinam, G.; Gautam, A.; Singh, G.; Swapnil; Mishra, K.; Mallick, S. Nickel and Cadmium Phytoextraction Efficiencies of Vetiver and Lemongrass Grown on Ni–Cd Battery Waste Contaminated Soil: A Comparative Study of Linear and Nonlinear Models. *J. Environ. Manag.* **2021**, *295*, 113144. [[CrossRef](#)]
34. Walkley, A.; Black, I.A. An Examination of the Degtjareff Method for Determining Soil Organic Matter, and a Proposed Modification of the Chromic Acid Titration Method. *Soil Sci.* **1934**, *37*, 29–38. [[CrossRef](#)]
35. Bharti, M.; Kamboj, N.; Kamboj, V.; Bisht, A.; Kumar, A. Dynamics of Soil Cationic Micronutrients in Different Land Use Systems in Lower Shiwalik Region of Uttarakhand, India. In *Environmental Pollution and Natural Resource Management*; Springer Proceedings in Earth and Environmental Sciences Series; Springer: Cham, Switzerland, 2022; pp. 185–199.

36. Fathabad, A.E.; Shariatifar, N.; Moazzen, M.; Nazmara, S.; Fakhri, Y.; Alimohammadi, M.; Azari, A.; Mousavi Khaneghah, A. Determination of Heavy Metal Content of Processed Fruit Products from Tehran's Market Using ICP-OES: A Risk Assessment Study. *Food Chem. Toxicol.* **2018**, *115*, 436–446. [[CrossRef](#)] [[PubMed](#)]
37. Kanwal, A.; Farhan, M.; Sharif, F.; Hayyat, M.U.; Shahzad, L.; Ghafoor, G.Z. Effect of Industrial Wastewater on Wheat Germination, Growth, Yield, Nutrients and Bioaccumulation of Lead. *Sci. Rep.* **2020**, *10*, 11361. [[CrossRef](#)] [[PubMed](#)]
38. Ismail, N.I.; Abdullah SR, S.; Idris, M.; Hasan, H.A.; Halmi MI, E.; Al Sbani, N.H.; Jehawi, O.H. Simultaneous Bioaccumulation and Translocation of Iron and Aluminium from Mining Wastewater by *Scirpus Grossus*. *Desalination Water Treat.* **2019**, *163*, 133–142. [[CrossRef](#)]
39. Eid, E.M.; Shaltout, K.H.; Alamri, S.A.M.; Sewelam, N.A.; Galal, T.M.; Brima, E.I. Prediction Models for Evaluating Heavy Metal Uptake by *Pisum Sativum* L. in Soil Amended with Sewage Sludge. *J. Environ. Sci. Health Part A* **2020**, *55*, 151–160. [[CrossRef](#)]
40. Galal, T.M.; Eid, E.M.; Dakhil, M.A.; Hassan, L.M. Bioaccumulation and Rhizofiltration Potential of *Pistia stratiotes* L. for Mitigating Water Pollution in the Egyptian Wetlands. *Int. J. Phytoremediat.* **2018**, *20*, 440–447. [[CrossRef](#)] [[PubMed](#)]
41. Sen, S.; Nandi, S.; Dutta, S. Application of RSM and ANN for Optimization and Modeling of Biosorption of Chromium(VI) Using Cyanobacterial Biomass. *Appl. Water Sci.* **2018**, *8*, 148. [[CrossRef](#)]
42. AL-Huqail, A.A.; Kumar, P.; Abou Fayssal, S.; Adelodun, B.; Širić, I.; Goala, M.; Choi, K.S.; Taher, M.A.; El-Kholy, A.S.; Eid, E.M. Sustainable Use of Sewage Sludge for Marigold (*Tagetes erecta* L.) Cultivation: Experimental and Predictive Modeling Studies on Heavy Metal Accumulation. *Horticulturae* **2023**, *9*, 447. [[CrossRef](#)]
43. Kyzioł, J. Effect of Physical Properties and Cation Exchange Capacity on Sorption of Heavy Metals onto Peats. *Pol. J. Environ. Stud.* **2002**, *11*, 713–718.
44. World Health Organization. *WHO Permissible Limits of Heavy Metals in Soil and Plants*; World Health Organization: Geneva, Switzerland, 1996.
45. Chowdhury, K.I.A.; Nurunnahar, S.; Kabir, M.L.; Islam, M.T.; Baker, M.; Islam, M.S.; Rahman, M.; Hasan, M.A.; Sikder, A.; Kwong, L.H.; et al. Child Lead Exposure near Abandoned Lead Acid Battery Recycling Sites in a Residential Community in Bangladesh: Risk Factors and the Impact of Soil Remediation on Blood Lead Levels. *Environ. Res.* **2021**, *194*, 110689. [[CrossRef](#)]
46. Ogundiran, M.B.; Osibanjo, O. Mobility and Speciation of Heavy Metals in Soils Impacted by Hazardous Waste. *Chem. Speciat. Bioavailab.* **2009**, *21*, 59–69. [[CrossRef](#)]
47. Orjiakor, P.; Atuanya, E. Effects of Automobile Battery Wastes on Physicochemical Properties of Soil in Benin City, Edo State. *Glob. J. Pure Appl. Sci.* **2015**, *21*, 129. [[CrossRef](#)]
48. Ariyachandra, S.P.; Alwis, I.S.; Wimalasiri, E.M. Phytoremediation Potential of Heavy Metals by *Cyperus rotundus*. *Rev. Agric. Sci.* **2023**, *11*, 20–35. [[CrossRef](#)]
49. Garba, S.T.; Guduusu, M.; Inuwa, L.B. Accumulation Ability of the Native Grass Species, *Cyperus rotundus* for the Heavy Metals; Zinc (Zn), Cadmium (Cd), Nickel (Ni) and Lead (Pb). *Int. Res. J. Pure Appl. Chem.* **2018**, *17*, 1–15. [[CrossRef](#)]
50. Bordoloi, S.; Basumatary, B. A Study on Degradation of Heavy Metals in Crude Oil-Contaminated Soil Using *Cyperus rotundus*. In *Phytoremediation*; Springer International Publishing: Cham, Switzerland, 2016; pp. 53–60; ISBN 9783319418117.
51. Jahan-Nejati, S.; Jowkar-Tangkarami, M.; Taei-Semiromi, J. *Cyperus rotundus*: A Safe Forage or Hyper Phytostabilizer Species in Copper Contaminated Soils. *Int. J. Phytoremediat.* **2021**, *23*, 1212–1221. [[CrossRef](#)]
52. Tripathy, A.P.; Dixit, P.K.; Panigrahi, A.K. Impact of Effluent of Pulp & Paper Industry on the Flora of River Basin at Jaykaypur, Odisha, India and Its Ecological Implications. *Environ. Res.* **2022**, *204*, 111769. [[CrossRef](#)] [[PubMed](#)]
53. DalCorso, G.; Fasani, E.; Manara, A.; Visioli, G.; Furini, A. Heavy Metal Pollutions: State of the Art and Innovation in Phytoremediation. *Int. J. Mol. Sci.* **2019**, *20*, 3412. [[CrossRef](#)] [[PubMed](#)]
54. Khandare, R.V.; Watharkar, A.D.; Pawar, P.K.; Jagtap, A.A.; Desai, N.S. Hydrophytic Plants *Canna Indica*, *Epipremnum Aureum*, *Cyperus Alternifolius* and *Cyperus rotundus* for Phytoremediation of Fluoride from Water. *Environ. Technol. Innov.* **2021**, *21*, 101234. [[CrossRef](#)]
55. Halder, L.; Arce, L.D.; Yllano, O.B. Bioaccumulation and Bioconcentration of Pb in the Tissues of Eight Weed Species. *J. Int. Sch. Conf.* **2016**, *1*, 14–18.
56. Khan, A.M. Accumulation, Uptake and Bioavailability of Rare Earth Elements (REEs) in Soil Grown Plants from Ex-Mining Area in Perak, Malaysia. *Appl. Ecol. Environ. Res.* **2017**, *15*, 117–133. [[CrossRef](#)]
57. Shakya, K.; Chettri, M.K.; Sawidis, T. Impact of Heavy Metals (Copper, Zinc, and Lead) on the Chlorophyll Content of Some Mosses. *Arch. Environ. Contam. Toxicol.* **2008**, *54*, 412–421. [[CrossRef](#)]
58. Zeeshan, M.; Ahmad, W.; Hussain, F.; Ahamd, W.; Numan, M.; Shah, M.; Ahmad, I. Phytostabalization of the Heavy Metals in the Soil with Biochar Applications, the Impact on Chlorophyll, Carotene, Soil Fertility and Tomato Crop Yield. *J. Clean. Prod.* **2020**, *255*, 120318. [[CrossRef](#)]
59. Rai, R.; Agrawal, M.; Agrawal, S.B. Impact of Heavy Metals on Physiological Processes of Plants: With Special Reference to Photosynthetic System. In *Plant Responses to Xenobiotics*; Springer: Singapore, 2016; pp. 127–140. ISBN 9789811028601.
60. Rajput, V.D.; Harish; Singh, R.K.; Verma, K.K.; Sharma, L.; Quiroz-Figueroa, F.R.; Meena, M.; Gour, V.S.; Minkina, T.; Sushkova, S. Recent Developments in Enzymatic Antioxidant Defence Mechanism in Plants with Special Reference to Abiotic Stress. *Biology* **2021**, *10*, 267. [[CrossRef](#)] [[PubMed](#)]

61. Dudonné, S.; Vitrac, X.; Coutière, P.; Woillez, M.; Mérillon, J.M. Comparative Study of Antioxidant Properties and Total Phenolic Content of 30 Plant Extracts of Industrial Interest Using DPPH, ABTS, FRAP, SOD, and ORAC Assays. *J. Agric. Food Chem.* **2009**, *57*, 1768–1774. [[CrossRef](#)] [[PubMed](#)]
62. Ighodaro, O.M.; Akinloye, O.A. First Line Defence Antioxidants—Superoxide Dismutase (SOD), Catalase (CAT) and Glutathione Peroxidase (GPX): Their Fundamental Role in the Entire Antioxidant Defence Grid. *Alex. J. Med.* **2018**, *54*, 287–293. [[CrossRef](#)]
63. Jena, A.B.; Samal, R.R.; Bhol, N.K.; Duttaroy, A.K. Cellular Red-Ox System in Health and Disease: The Latest Update. *Biomed. Pharmacother.* **2023**, *162*, 114606. [[CrossRef](#)]
64. Adejumo, S.A.; Tiwari, S.; Thul, S.; Sarangi, B.K. Evaluation of Lead and Chromium Tolerance and Accumulation Level in *Gomphrena Celosoides*: A Novel Metal Accumulator from Lead Acid Battery Waste Contaminated Site in Nigeria. *Int. J. Phytoremediat.* **2019**, *21*, 1341–1355. [[CrossRef](#)]
65. Zhao, B.; Zhu, W.; Hao, S.; Hua, M.; Liao, Q.; Jing, Y.; Liu, L.; Gu, X. Prediction Heavy Metals Accumulation Risk in Rice Using Machine Learning and Mapping Pollution Risk. *J. Hazard. Mater.* **2023**, *448*, 130879. [[CrossRef](#)]
66. Kumar, P.; Kumar, V.; Singh, J.; Kumar, P. Electrokinetic Assisted Anaerobic Digestion of Spent Mushroom Substrate Supplemented with Sugar Mill Wastewater for Enhanced Biogas Production. *Renew. Energy* **2021**, *179*, 418–426. [[CrossRef](#)]
67. Chen, P.; Zhang, H.-M.; Yao, B.-M.; Chen, S.-C.; Sun, G.-X.; Zhu, Y.-G. Bioavailable Arsenic and Amorphous Iron Oxides Provide Reliable Predictions for Arsenic Transfer in Soil-Wheat System. *J. Hazard. Mater.* **2020**, *383*, 121160. [[CrossRef](#)]
68. Chiou, W.-Y.; Hsu, F.-C. Copper Toxicity and Prediction Models of Copper Content in Leafy Vegetables. *Sustainability* **2019**, *11*, 6215. [[CrossRef](#)]
69. Ijadi Bajestani, M.; Mousavi, S.M.; Shojaosadati, S.A. Bioleaching of Heavy Metals from Spent Household Batteries Using *Acidithiobacillus Ferrooxidans*: Statistical Evaluation and Optimization. *Sep. Purif. Technol.* **2014**, *132*, 309–316. [[CrossRef](#)]

Disclaimer/Publisher’s Note: The statements, opinions and data contained in all publications are solely those of the individual author(s) and contributor(s) and not of MDPI and/or the editor(s). MDPI and/or the editor(s) disclaim responsibility for any injury to people or property resulting from any ideas, methods, instructions or products referred to in the content.